Journal of Applied Polymer Science

Structure and Properties of Ultra-High Molecular Weight Bisphenol A Polycarbonate Synthesized by Solid-State Polymerization in Amorphous Microlayers

In Hak Baick,[1] Woo Jic Yang,[1] Yun Gyong Ahn,[2] Kwang Ho Song,[3] Kyu Yong Choi[1]

[1]Department of Chemical and Biomolecular Engineering, University of Maryland, Maryland 20742

[2]Korea Basic Science Institute, Seoul Center, Seongbuk-Gu, Seoul 136-701, Korea

[3]Department of Chemical and Biological Engineering, Korea University, Anam-dong, Seongbuk-Gu, Seoul 136-713, Korea

Correspondence to: K. Y. Choi (E-mail: choi@umd.edu)

ABSTRACT: The structure and properties of ultrahigh molecular weight polycarbonate synthesized by solid-state polymerization in micro-layers (SSP_m) are reported. A low molecular weight prepolymer derived from the melt transesterification of bisphenol A and diphenyl carbonate as a starting material was polymerized to highly amorphous and transparent polycarbonate of molecular weight larger than 300,000 g mol^{-1} in the micro-layers of thickness from 50 nm to 20 μm. It was observed that when the polymerization time in micro-layers was extended beyond conventional reaction time, insoluble polymer fraction increased up to 95%. Through the analysis of both soluble and insoluble polymer fractions of the high molecular weight polycarbonate by ^1H NMR spectroscopy and pyrolysis-gas chromatography mass spectrometry (Py-GC/MS), branches and partially crosslinked structures have been identified. The thermal, mechanical and rheological properties of the ultra-high molecular weight nonlinear polycarbonates synthesized in this study have been measured by differential scanning calorimetry (DSC), dynamic mechanical analysis (DMA), and rheometry. The nonlinear chain structures of the polymer have been found to affect the polymer's thermal stability, mechanical strength, shear thinning effect, and elastic properties. © 2014 Wiley Periodicals, Inc. J. Appl. Polym. Sci. **2015**, *132*, 41609.

KEYWORDS: crosslinking; mechanical properties; polycarbonates; polycondensation; synthesis and processing

Received 29 July 2014; accepted 3 October 2014

DOI: 10.1002/app.41609

INTRODUCTION

Linear bisphenol A polycarbonate (BPAPC) is one of the most widely used thermoplastics for many engineering applications in automotive, electronic display, data storage, medical, environmental, energy, and aerospace industries due to its high glass transition temperature (~150°C), excellent optical clarity, and high impact resistance.[1–3] BPAPC is also known to have relatively poor solvent resistance, low surface hardness and low scratch resistance, which can be improved by modifying the polymer chain structure via crosslinking using multifunctional comonomers.[4] In recent years, branched and crosslinked PCs are of interest to industry because they have some new potential applications such as a binder in photoconductors and an optical component in multilayer structures.[5,6] In a melt polycondensation process of BPAPC, the addition of alkali metal and alkaline compounds to the reaction mixture without using trifunctional branching agents has been reported to induce the formation of a small amount of branched polycarbonates by the thermal rearrangement reaction known as Fries rearrangement reaction, leading to about 0.017–0.043 branching units per chain.[7,8] If the weight average molecular weight per branch arm is higher than the critical molecular weight for entanglements (e.g., $M_c = 4000–4800$ g mol^{-1}), the polymer is called the long-chain branched polymer.[9] The presence of branched units influences the rheological properties and the crystallization behavior of polycarbonates. For instance, while high molecular weight linear polycarbonate melt is not easy to process, long-chain branched PCs are relatively easier to process for injection molding. The higher mobility of polymer chains in long-chain branched polycarbonates compared to that of linear polycarbonates was reported through dielectric relaxation analysis.[10] Higher melt elasticity and shear rate sensitivity were also observed while mechanical properties were not changed much for a wide range of compositions (0–100 wt % of branched BPAPC) of linear and branched BPAPC blends in commercially available long-chain branched polycarbonates.[10]

Crosslinking reactions in polycarbonate have also been reported to occur when high temperature degradation of polycarbonate

is carried out under high vacuum conditions.[11,12] At typical melt polycondensation temperature, (e.g., 260–280°C), the formation of crosslinked polycarbonate is generally quite small.[13,14] The formation of crosslinking at high temperature thermal degradation reactions was attributed to the effective removal of phenol.[11,12,15] The structures of insoluble polycarbonates were investigated using various analytical techniques including NMR, IR, and GC-MS in the past.[16–18] In particular, the pyrolysis-gas chromatography mass spectrometry (Py-GC/MS) in presence of tetramethylammonium hydroxide (TMAH) has been found to be effective in characterizing the crosslinking structure of the BPAPC.[16] The formation of insoluble fractions in polycarbonate synthesis is believed to be caused by the thermal rearrangement of the carboxyl group into a pendant carboxyl group, which undergoes further esterification, and hydrogen abstraction from methyl and aromatic protons to generate radicals followed by radical recombination, leading to the crosslinked chains.

In general, high molecular weight BPAPC (up to 50,000 g mol^{-1}) can be produced by conventional solid-state polymerization (SSP) in a continuous flow reactor process using spherical particles (100–1000 μm) of BPAPC prepolymers obtained from direct melt polycondensation processes.[19–21] The polymerization rate is quite slow because the chain mobility is low at the solid-state temperature that is above the glass transition temperature but much below the melting temperature. Polymer particles or pellets are relatively large to prevent partial melting and agglomeration in a continuous flow solid-state polymerization reactor. Theoretical modeling of a single SSP particle used in such conventional SSP process has shown that significant diffusion resistance is present in the transport of phenol (byproduct of polycondensation of BPAPC) from the particle interior to the external surface of the particle.[22,23] In our recent work, we have reported that when BPAPC is polymerized in thin micro-layers under solid-state polymerization conditions, very high molecular weight polycarbonate ($M_w > 100{,}000$ g mol^{-1}) can be obtained in short reaction time.[24]

In this study, we report new experimental results that highly crosslinked BPAPC are formed in micro-layers by solid-state polymerization without using any external crosslinking agent when the reaction time is significantly extended beyond typical solid-state polymerization time. The kinetic aspects of polymerization as well as the properties of these nonlinear polymers are reported.

EXPERIMENTAL

Materials

Amorphous low molecular weight (14,000 g mol^{-1}) BPAPC was used as a prepolymer for solid-state polymerization. A low molecular weight prepolymer ($M_w = 14{,}000$ g mol^{-1}) was prepared from semi-batch direct melt polycondensation of bisphenol A (BPA, 99.9%, Aldrich) and diphenyl carbonate (DPC, 99.9%, Aldrich) with lithium hydroxide monohydrate catalyst ($LiOH{\cdot}H_2O$, Aldrich).[14,25] The end group mole ratio of the prepolymer ([—OCO—C_6H_5]/[—OH]) was 0.8. For solvent casting, a predetermined amount of prepolymer was dissolved in chloroform at room temperature. The micro-layers of prepolymer were prepared by solvent casting and spin coating techniques. The silica substrate (2.5 cm × 7.5 cm) was cleaned with acetone and methanol for 5–10 min, rinsed with deionized water, and dried under nitrogen gas flow. To prepare 5- to 20-μm-thick polymer micro-layers, the silica substrate was preheated before solvent casting to prevent partial crystallization of polymer microlayers. Sub-micrometer amorphous polymer-layer samples (50–1020 nm) were prepared by spin coating at 2000 rpm. The amorphous micro-layers were dried in a fume hood for 2 h at ambient temperature and pressure. A high temperature vacuum oven was modified and used as a reaction chamber (Fisher Scientific™ Isotemp™ Model 281A Vacuum Oven, 0.65 cu. Ft.) for the solid-state polymerization. The solid-state polymerization experiments were carried out at 230°C and 10 mm Hg. The amount of insoluble polymers was measured as follows: samples (0.5 g) at each reaction time were dissolved in a large amount of chloroform (500 mL) and the soluble and insoluble polymer fractions were separated via filtration using a 0.2-μm pore size membrane followed by washing with a solvent (chloroform) at least 10 times and weighted using the gravimetic method. Only the soluble fraction was used to measure the molecular weight using GPC.

Polymer Analysis

The molecular weight and molecular weight distribution (MWD) of the prepolymer and soluble portion of the high molecular weight polymer products were measured by a gel permeation chromatography (GPC, Waters) system equipped with PLgel 10 μm MIXED-B columns (Polymer Laboratories) and a UV detector (Waters 484). Chloroform was used as a mobile phase and narrow MWD polystyrene standards were used for the universal column calibration. The polycarbonate molecular architecture was analyzed using high resolution ^{1}H NMR spectroscopy (Bruker AV III spectrometer at 600 MHz) and Py-GC/MS (Frontier Lab PY-2020iD pyrolyzer). For the ^{1}H NMR spectroscopy analysis, polymer samples taken from the solid-state polymerization experiments were dissolved in deuterated chloroform ($CDCl_3$). For the analysis of insoluble gel fractions, Py-GC/MS was used equipped with an Agilent GC/MS system composed of an Agilent 6890 gas chromatograph and an Agilent 5975i mass spectrometer for analysis. An aqueous solution (25 wt %) of tetramethylammonium hydroxide [$(CH_3)_4NOH$; TMAH] (Aldrich) was used as the reagent for methylation of the product samples.

The thermal analysis of SSP_m samples was conducted by differential scanning calorimetry (DSC, TA Instrument Q1000). About 5–6 mg of polymer samples were taken and sealed in a TA Instrument Hermetic aluminum DSC cans. A temperature range of 10–300°C was used to cover both T_g and T_m with a scan rate of 10°C min^{-1}. The first cycle of heating and cooling was done to remove solvent effects and former thermal history and data from the second cycle was collected to investigate the thermal properties of SSP_m PC samples.

For the dynamic mechanical analysis (DMA, TA Instrument Q800), 40- and 200-μm-thick samples were prepared by stacking and fusing 10-μm-thick amorphous micro-layers using a Carver Laboratory Heat Press at 200°C. The 40-μm-thick samples were used to obtain strain–stress curves and 200-μm-thick

samples were used for the dynamic mechanical analysis using a temperature sweep mode. Different sample thicknesses were used for the two different analyses due to maximum and minimum static force limits of the instrument. Rectangular shaped samples (5.0 mm (L) × 5.3 mm (W)) were prepared using TA Instrument sample cutter. For the tensile measurement, analysis conditions were set as follows: initial strain at 0.1%; constant temperature at 25°C; extension rate at 40 μm min^{-1}; Poisson's ratio of 0.37. Dislocation of samples was applied until the micro-layer samples fractured. A temperature sweep was used under a nitrogen environment in order to investigate the glass transition temperature, storage modulus, and phase lag ($\tan\delta$). The initial strain was set to 0.5% and a preload force of 0.01N was applied with a constant frequency of 1 Hz. The analysis was carried out from 20 to 300°C. However, the final data point for each sample varied depending on their disentanglement characteristics. The temperature was raised in increments of 4°C with 2 min given at each analysis temperature to equilibrate the sample at target temperatures.

Rheological properties of the polymer samples were measured using a rotational rheometer (RSA III Analyzer (Rheometric Scientific)) with a parallel-plate (25 mm in diameter) geometry with a sample thickness of 400–500 μm. A strain of 5% was used as all samples were in the linear viscoelastic regime. The analysis temperature was set to 260°C for rheological analysis. Dynamic storage modulus (G'), loss shear modulus (G''), and complex viscosity (η^*) were obtained at a frequency range of 0.01–100 rad s^{-1} under continuous nitrogen gas flow to prevent any unwanted degradation or side reactions.

RESULTS AND DISCUSSION

Solid State Polymerization in Amorphous Microlayers (SSP_m)

In the solid-state polymerization of BPAPC in amorphous micro-layers (SSP_m), the reaction byproduct (phenol) can be removed more effectively than in micro-particles and hence high molecular weight is obtained in short reaction time.[24] A small amount of casting solvent left in the micro-layer can also act as a plasticizer to facilitate the movement of chain segments at the reaction temperature. It has been found that the resulting high molecular weight polymer that was soluble in chloroform contained branched and partially crosslinked polymers. Branched polycarbonates can be formed via Kolbe–Schmitt rearrangement reaction or the Fries rearrangement reaction where carbonate groups in linear BPAPC can rearrange to form pendant carboxyl groups, ortho to an ether link, and through ester exchange reaction with another BPAPC chain, long chain branched structures can be formed. Crosslinked structures can also be formed via radical recombination reactions. A small amount of radical species can be formed from homolytic scission of carbonate groups between the oxygen and carbonyl group in BPAPC at high temperatures and from hydrogen abstraction, which result in methylene radicals on carbonate groups and phenoxy radicals, respectively.[8,16] The byproduct, phenol, is a known radical scavenger.[26,27] Thus, in the conventional SSP with relatively large spherical particles or pellets where diffusional transport of phenol is rather slow, high concentration of phenol in the polymer particles may prohibit the formation of crosslinked PC but in the SSP_m, phenol is almost instantly removed from the micro-layers, making the recombination of macro-radical species more favorable to form crosslinked chain structures than in conventional solid-state polymerization.

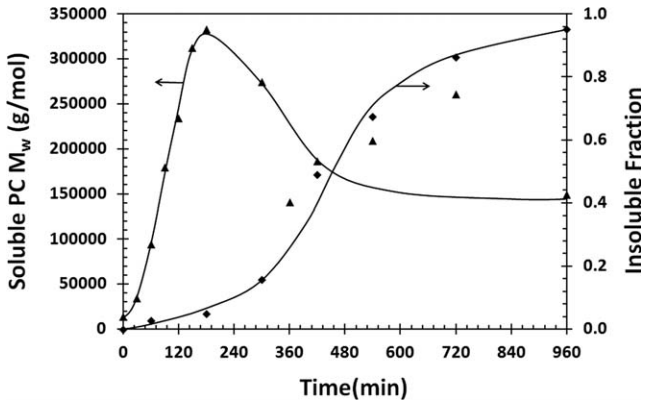

Figure 1. Molecular weights of soluble polycarbonate fractions (▲) and insoluble polymer fractions (◆) with the reaction time for 10-μm-thick amorphous micro-layers (Prepolymer: M_w =14 k g mol^{-1}, P = 10 mmHg, T = 230°C). Lines are added to guide the eyes.

Figure 1 shows the experimental results for the solid-state polymerization in micro-layers of 10 μm thickness at 230°C and 10 mmHg. Here, the molecular weight data shown in Figure 1 are for the soluble fractions only because it was not possible to measure the molecular weight of the insoluble polymer fractions by gel permeation chromatography. We can observe that the polymer molecular weight rises rapidly to about 340,000 g mol^{-1} before it starts to decrease and settles at about 150,000 g mol^{-1}. Figure 1 also shows that the weight fraction of insoluble fraction increases with time. Also, notice that after 960 min of reaction, the insoluble fraction reaches as high as 95%. The decrease in molecular weight after reaching the maximum is thought to be caused by the involvement of high molecular weight chain segments in crosslinking reactions to form insoluble fractions. Recall that the end group mole ratio of the prepolymer ([—OCO—C_6H_5]/[—OH]) was 0.8 that is quite off from the stoichiometric ratio, which is considered as a necessary condition to obtain high molecular weight linear condensation polymer in Flory's sense. The fast increase to very high molecular weights such as shown in Figure 1 was attributed to the rapid removal of phenol and the formation of nonlinear chain structures (branching and partial crosslinking).[24] It is also interesting to note that the molecular weight of soluble fractions becomes quite constant at about 150,000 g mol^{-1} even after the insoluble fraction has reached 95%.

The low concentration of phenol in the amorphous micro-layer allows for the extended survival time for radicals and hence radical recombination reactions are believed to be responsible for the formation of insoluble crosslinked polymers. Longer polymer chains have a higher probability for the formation of radical sites thus a higher chance of recombination of macro-radical species is expected. In our previous study, it was shown that after the early stages of the reaction (<30 min), the concentrations of phenolic hydroxyl groups ([—C_6H_4—OH]) and phenyl carbonatete groups

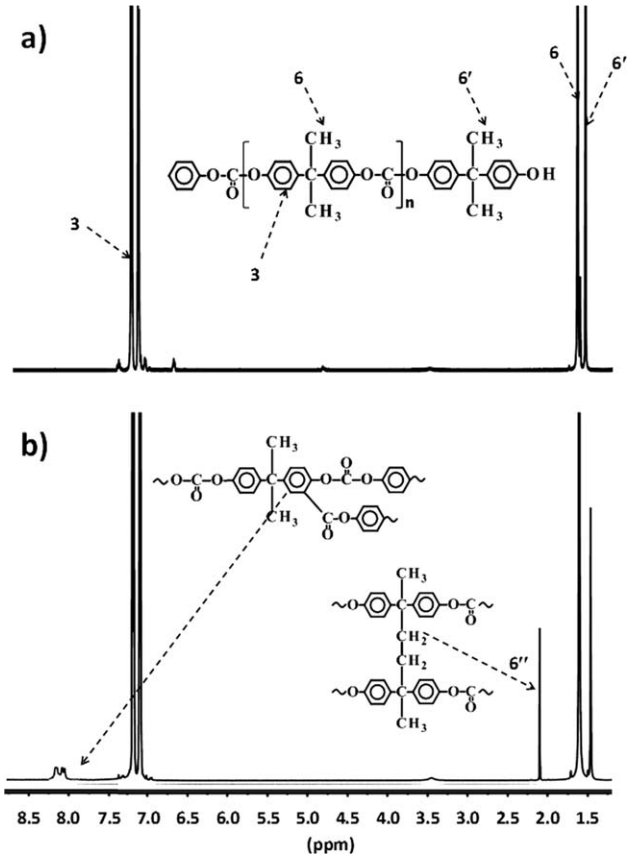

Figure 2. ^{1}H NMR spectroscopic analysis of the polymer: (a) prepolymer, (b) soluble fraction at the reaction time of 960 min ($T = 230°C$, layer thickness = 10 μm).

([—OCO—C_6H_5]) decreased to insignificant levels, indicating that standard linear step-growth polymerization were negligible and contributed little or none to further increase in molecular weight.[24] Therefore, the molecular weight increase to 340,000 g mol^{-1} after 180-min reaction is due to the formation of nonlinear polymer chains. When a small fraction of insoluble gels is produced in conventional high temperature melt polycondensation processes, the product exhibits discoloration (e.g., yellowish or dark brown).[11,12,15,17,18] However, the polycarbonate obtained in our experiments, even after 960 min (95% insoluble) of reaction, was transparent with no discoloration.

Characterization of the Polymer Structures

The chain structures of the polymer (i.e., branched and cross-linked structures) were identified using ^{1}H NMR spectroscopy and pyrolysis gas chromatography Mass Spectrometry (Py-GC/MS).

Structures of Soluble Fractions. Figure 2 shows the ^{1}H-NMR spectroscopy data of prepolymer (a), and high molecular weight polycarbonate in the soluble fraction obtained at 960 min (b). For the soluble polymer, the aromatic regions (peak at 8.0–8.1 ppm) for phenyl salicylate phenyl carbonate (PhSALPhC) and ethyl protons on the linkage of crosslinked structure were confirmed. The mole fraction of crosslinkage was 0.0633 which was estimated using the area intensity of methyl protons and ethyl protons in repeating units and crosslinkages as follows:

$$\text{Mole fraction of cross-linkages} = \frac{\text{peak6}''/4}{\text{peak6}/6 - \text{peak6}''/4 + \text{peak6}''/2} \quad (1)$$

The mole fractions of crosslinks in the soluble fraction were 3.55×10^{-4} and 4.26×10^{-2} at 30 and 180 min, respectively (see Table I). At early stages of the reaction, crosslinks increased about two orders of magnitude. However, the mole fraction of crosslinks in the soluble fraction did not change much after 180 min of reaction time probably due to the insolubility of highly crosslinked polymer chains (^{1}H NMR spectroscopy analysis was limited to the soluble fraction only). The data in Table I seem to indicate that the insoluble gel formation occurred around the crosslink mole fraction of between 4.26×10^{-2} and 6.33×10^{-2}. The molecular weight of soluble polymer chains decreased after 180 min of reaction time at 230°C and the insoluble gel fraction increased rapidly after 300 min of reaction time (see Figure 1).

Molecular Structures of Insoluble Fractions. The Py-GC/MS analysis is an effective technique for the qualitative analysis of branched and cross-linked polycarbonate.[16,28] Through reactive pyrolysis of insoluble gels at a high temperature (400°C) in the presence of tetramethylammonium hydroxide (TMAH), linear, branched and cross-linked polymer chains are selectively

Table I. Sample Weight Average Molecular Weight of Soluble PCs, Insoluble Fraction (Mass Fraction), Polydispersity, and Mole Fraction of Crosslinkage with the Reaction Time for 10-μm-thick Amorphous Microlayers (Prepolymer Molecular Weight = 14k g mol^{-1}, $P = 10$ mmHg, $T = 230°C$)

	10 μm Amorphous microlayers (SSP_m at 230°C)				
Sample ID	Reaction time (min)	M_w in soluble frac. (g mol^{-1})	Insoluble fraction	Polydispersity	Mole fraction of crosslinks[a]
PRE-0	0	14,000	0	1.97	0
SSPM-30	30	34,000	-	2.26	3.55×10^{-4}
SSPM-60	60	94,000	0.03	2.32	8.89×10^{-4}
SSPM-180	180	333,000	0.05	2.57	4.26×10^{-2}
SSPM-420	420	187,000	0.49	3.22	6.28×10^{-2}
SSPM-960	960	149,000	0.95	5.46	6.33×10^{-2}

[a] These values were obtained by ^{1}H NMR analysis (soluble fraction only).

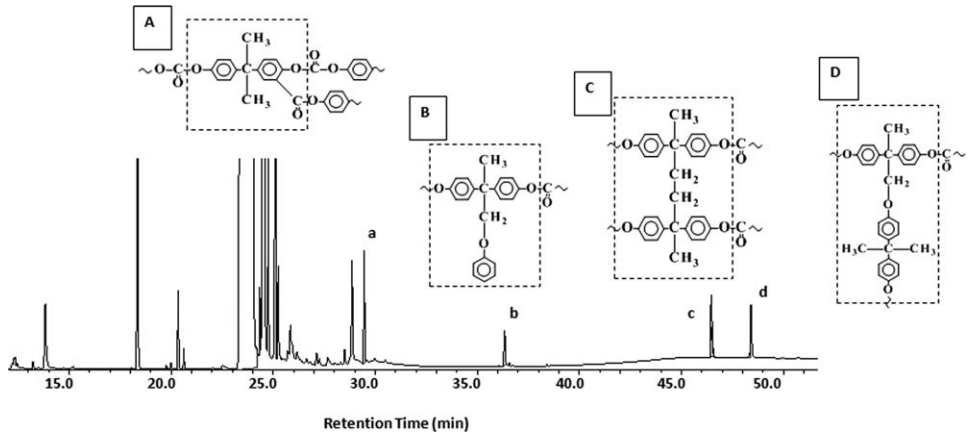

Figure 3. Pyrogram of insoluble gel obtained at the reaction time of 960 min ($T = 230°C$, layer thickness = 10 μm).

decomposed to methyl derivatives of the components which are detected by mass spectrometry. The program of Py-GC/MS in Figure 3 shows that the insoluble gel consists of branched and cross-linked structures (structure C, D). Structure A (peak a) can be formed via thermal rearrangement reactions (Fries or Kolbe–Schmitt rearrangement reactions) while radical recombination reactions of macro-radical species lead to structure B, C, and D (peaks b, c, d).[16,28] According to the structures B–D obtained through radical recombination, two macro-radical species can be formed during the SSP_m process, methylene radical via hydrogen abstraction from the methyl group and phenoxy radical through chain scission at the carbonate group. Two methylene radical species may form Structure C that corresponds to peak c while the combination of methylene radical and phenoxy radical species produce Structure D (peak d).[16]

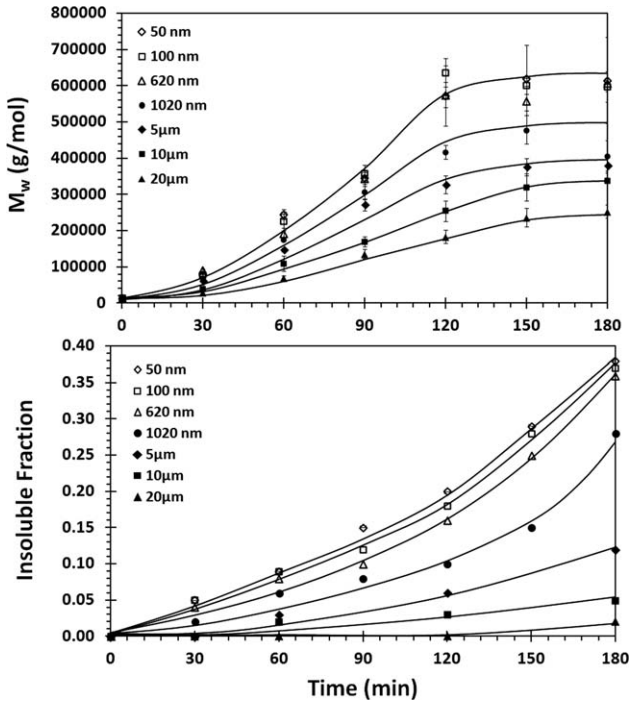

Figure 4. (a) Effect of the amorphous micro-layer thickness on the evolution of the polymer molecular weight with the reaction time and (b) formation of insoluble fraction in amorphous micro-layers depending on thickness ($T = 230°C$, $P = 10$ mmHg, Prepolymer B-14k). Lines were added to guide the eyes only.

Effects of Layer Thickness

The effect of micro-layer thickness on the molecular weight and insoluble gel fraction in SSP_m is illustrated in Figure 4 for the micro-layer thickness ranging from 50 nm to 20 μm up to 180 min of reaction time. Thinner layers of 50–1020 nm were measured using AFM in tapping mode and the height images were used to obtain precise thickness measurements for each sample. The thicknesses of micrometer scale samples were measured using a Mitutoyo micrometer (Japan). All amorphous micro-layer samples maintained transparency during the entire period of polymerization. When the micro-layer thickness was larger than 30 μm, partial crystallization occurred during the solvent casting procedure and thus we limited the maximum thickness to 20 μm to maintain the transparency of the micro-layers.

Figure 4(a) shows that the molecular weight reaches an asymptotic maximum value of about 600,000 g mol^{-1} when the micro-layer thickness is 620 nm or smaller. According to the simulation model of the SSP_m process reported in our previous article, the phenol concentration of micro-layers of thickness <1020 nm is approximately zero throughout the entire polymerization process.[24] Further, in the case of 10 and 20 μm samples, the phenol concentration is four to five orders of magnitude greater than that of nanometer scale samples during the first 180 min of polymerization. Thus, the phenol concentration, which depends on the layer thickness, has a strong effect on the molecular weight and insoluble fraction for the micrometer scale samples (5–20 μm). For the nanometer scale micro-layers (50–1020 nm), the thickness effect seems to be very small. It is to be noted that the MW values shown in Figure 4(a) are for the soluble fractions. As shown in Figure 4(b), the emergence of insoluble polymers was observed earlier as micro-layer thickness decreased. The insoluble gel fraction of 10 μm samples at 180 min is about 5% while the 50- to 620-nm-thick micro-layers show about 35%. The micro-layer thickness and insoluble fraction can be correlated experimentally by the

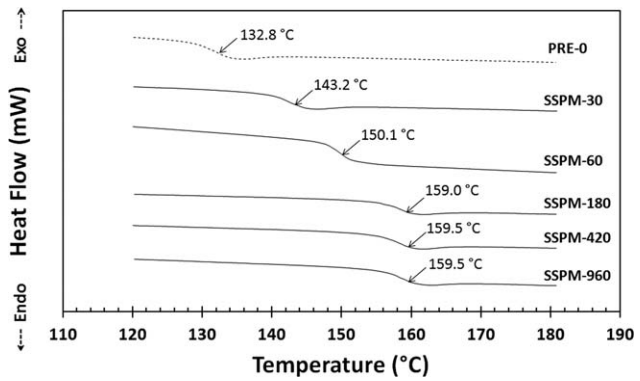

Figure 5. DSC thermograms of prepolymer and amorphous SSP_m PCs at different reaction times ($T = 230°C$, $P = 10$ mmHg).

equation $\log(\mathbf{y}) = -0.4743 - 6.65 \times 10^{-5}\ \mathbf{x}$, where $\mathbf{y}$ is the insoluble fraction and $\mathbf{x}$ is the micro-layer thickness in nanometers.

Properties of High Molecular Weight Nonlinear Polycarbonates

Thermal Properties. A differential scanning calorimetry (DSC) was used to measure the glass transition temperatures (T_g) of the high molecular weight amorphous micro-layer samples. Figure 5 shows the DSC thermograms of the prepolymer (PRE-0 in Table I) and amorphous micro-layers of 10 μm thickness synthesized at 230°C at different reaction times (SSPM-30 to 960 in Table I). The glass transition temperature of the low molecular weight linear prepolymer (PRE-0) is 132.8°C but the T_g increases with reaction time as both the polymer molecular weight and the insoluble fraction increase. After 180 min of reaction time (SSPM-180), T_g becomes constant at around 159°C which is higher than the reported T_g values of commercial linear BPAPC (e.g., 146°C (31,000 g mol^{-1}), 153°C (43,000 g mol^{-1})).[10,29,30] The presence of partially crosslinked polymer chains copresent with linear BPAPC chains is believed to increase the T_g because they would hinder the rotation of chain segments. At 180 min (SSPM-180), the insoluble fraction is about 5% and it rapidly increases after 300 min (see Figure 1). However, T_g does not seem to increase with the increase in the insoluble fraction. Although it is not shown here, the soluble and insoluble fractions of the sample SSPM-960 was separated using its solubility in chloroform and T_g for each fraction was measured. Both soluble and insoluble gel fractions have a glass transition temperature of around 159°C.

Mechanical Properties. The tensile properties of the polymers were measured by dynamic mechanical analysis (DMA) at 25°C. The 10 μm amorphous samples taken from different reaction times were stacked and melted (fused) to make 40-μm-thick films. The measured strain–stress curves are shown in Figure 6 for five different samples obtained at different reaction times. For comparison, the stress–strain curve for prepolymer (MW 14,000 g mol^{-1} (PRE-0)) was also analyzed, but the prepolymer sample fractured at a strain of 0.9%. The prepolymer samples were very brittle and it was difficult to prepare the test samples without cracking. The high MW amorphous SSP_m PCs showed a great degree of ductility as commonly seen in bisphenol A polycarbonates.[31,32] Tensile moduli of 340–1550 MPa were found for SSP_m samples, and the tensile modulus and the ultimate tensile strength increased as insoluble fractions increased. The increase of ultimate tensile strength is due to the increase in chain length and degree of crosslinking, indicating that a decrease in the rate of stress relaxation with crosslinking inhibits polymer chain flow.[4] Recall that Sample c (SSPM-180 in Table I) has the weight average molecular weight of 340,000 g mol^{-1} with 5% insoluble fraction (branched and partially crosslinked PCs) while Sample e (SSPM-960 in Table I) has nearly 95% insoluble PCs. The ultimate tensile strength and elongation of sample SSPM-960 were 69.5 MPa and 54.6%, respectively. Figure 6 shows that the ultimate elongation of SSP_m PCs increased until 180 min (sample c) and then decreased with a further increase in the reaction time, which results in higher insoluble fractions in the polymer. The decrease in ultimate elongation is a typical behavior of crosslinked polymers caused by the drop in the number of available polymer chain conformational states of crosslinked polymers.[33] Similar behavior as shown in Figure 6 was reported for the cross-linked benzocyclobutene-terminated polycarbonate.[4]

The results obtained from DMA temperature sweep tests for the prepolymer (PRE-0) and SSP_m PCs with different reaction times are given in Figure 7. Storage modulus versus temperature profiles were obtained using 200-μm-thick amorphous micro-layer samples which were prepared by fusing 10-μm-thick samples. SSP_m PC samples show different dynamic mechanical responses depending on their molecular weight and molecular structures. The second order transition of the prepolymer is 147.2°C. Compared to the T_g obtained from DSC analysis (see Figure 5), a value about 15°C higher was observed. The transition point increases until a reaction time of 180 min (SSPM-180) is reached and stabilizes at a temperature of around 164°C. Up to reaction time of 180 min (SSPM-180), there is a clear trend of increasing T_g, which can be attributed to the increase in chain length and degree of crosslinking. Sample SSPM-180, which has 5% insoluble fraction, exhibits roughly the same transition temperature observed in SSPM-420 (49% insoluble) and SSPM-960 (95% insoluble) samples. It seems that the onset of insoluble gel formation does not affect the second order transition of polymer chains. Compared to the mole fraction of crosslinks

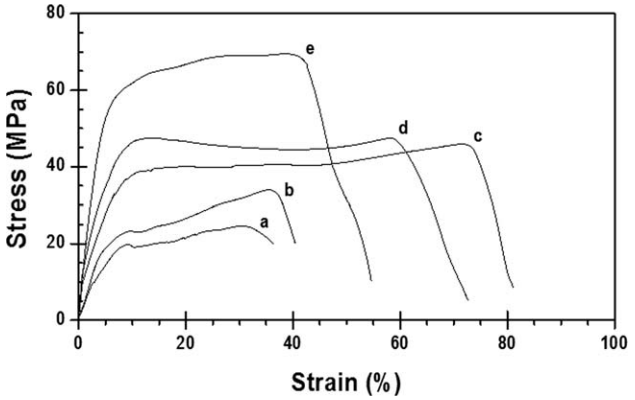

Figure 6. Strain–stress curves of SSPm PCs with reaction time: (a) SSPM-30, (b) SSPM-60, (c) SSPM-180, (d) SSPM-420, and (e) SSPM-960.

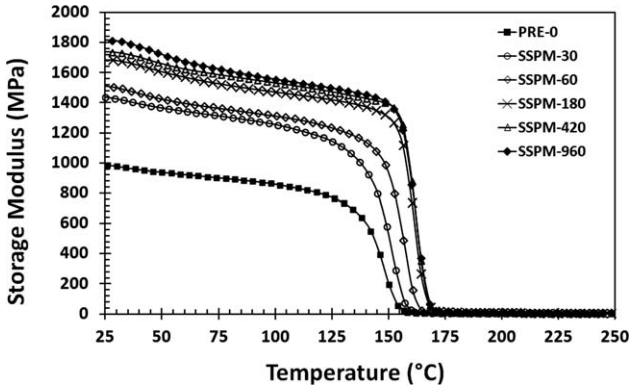

Figure 7. SSP$_m$ PCs storage modulus as a function of temperature at 1 Hz with initial strain at 0.5% and preload force at 0.01 N. SSP$_m$ PCs were obtained at reaction temperature of 230°C with 10 μm thickness microlayers: PRE-0 (-■-), SSPM-30 (-○-), SSPM-60 (-◇-), SSPM-180 (-×-), SSPM-420 (-△-), and SSPM-960 (-◆-).

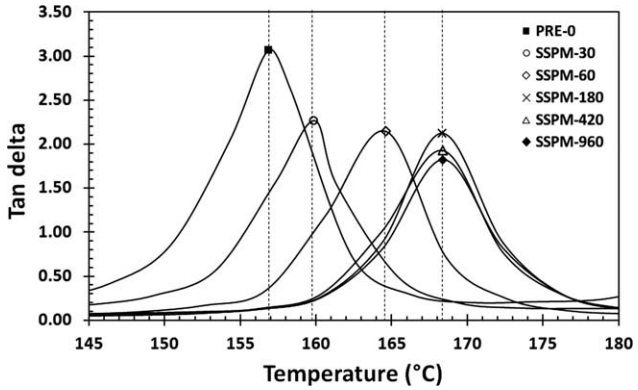

Figure 8. Loss tan δ as a function of temperature at 1 Hz with initial strain at 0.5% and preload force at 0.01*N*. Peak positions are marked as: PRE-0 (-■-), SSPM-30 (-○-), SSPM-60 (-◇-), SSPM-180 (-×-), SSPM-420 (-△-), and SSPM-960 (-◆-).

for sample SSPM-30, SSPM-60 shows a slight increase while SSPM-180 shows an increase of two orders of magnitude (see Table I), which has a significant impact on the second order transition. For the soluble fraction of SSPM-960, the mole fraction of crosslinks is 6.33×10^{-2} which is only slightly larger than the 180 min sample. After 180 min, the insoluble fraction increases rapidly while the T_g remains almost constant. This observation is consistent with the DSC results which shows that the T_g stabilizes around 159°C after 180 min (sample SSPM-180) (see Figure 5). At temperatures below the second order transition, the polymers are in a glassy state. In the glassy state, all samples show gradual decreases in storage moduli until the temperature reaches the glass transition. The storage modulus of the prepolymer (PRE-0) at the initial temperature (25°C) is about 1000 MPa and for SSPM-30, the initial storage modulus increases to 1450 MPa. Thus, only after the first 30 min of SSP$_m$, the storage modulus at 25°C increases significantly due to the increases in chain length and degree of crosslinking. Slight increments of the initial storage moduli are seen after 180 min of SSP$_m$ (SSPM-180). Sample SSPM-960, which has a 95% insoluble fraction, shows a storage modulus about 1.84 times higher than the low molecular weight linear prepolymer (sample PRE-0).

The analytical software (Universal Analysis® software version 4.5) was used to obtain the loss tangent (tan δ) curves as given in Figure 8. As discussed previously, the loss tangent curves also show an increase in second order transition up to SSP$_m$ reaction time of 180 min. Also, the peak height decreases as the reaction time of SSP$_m$ process increases, indicating that the energy loss (phase lag (δ)) becomes lower as molecular weight of polymer increases due to crosslinking. After the onset of insoluble gel formation (SSPM-180), the T_g remains nearly constant at 168.5°C. However, the decreasing peak height of the loss tangent curves indicates that the energy loss becomes smaller as the insoluble fraction increases (see SSPM-180, SSPM-420, and SSPM-960 in Figure 8).

Above the glass transition temperature, the polymers are in a rubbery state in which the polymer chains have full mobility and their entanglement network affects the behavior of the dynamic modulus.[34] Differences in molecular weights and molecular structures affect the polymer chain entanglements in this state. Above T_g, all samples show significant drops in storage moduli to values about three orders of magnitude lower as the stress relaxation of polymer chains become higher.[35] To see the different behaviors in the rubbery state, a logarithmic scale was applied to the storage modulus as given in Figure 9. With the prepolymer sample (PRE-0 in Figure 9 (■)), the storage modulus decreases as the temperature is raised and further temperature increments engenders the disentanglement of polymer chains at analysis temperatures higher than 230°C. As the SSP$_m$ process proceeds, the storage modulus increases, and for samples with a higher degree of crosslinking, the slope decreases to reach a plateau in the higher range of analysis temperatures, exhibiting elastic behavior in the rubbery state (see SSPM-960 in Figure 9). Thus, the partially crosslinked polymers (SSPM-960) containing high fractions of insoluble gel behave like typical thermosets.

Figure 10 shows the tan δ values as temperature is increased through rubbery state until the disentanglement of polymer chains occurred for each sample. For all samples, the loss tangent (δ) gradually increases as temperature increases indicating

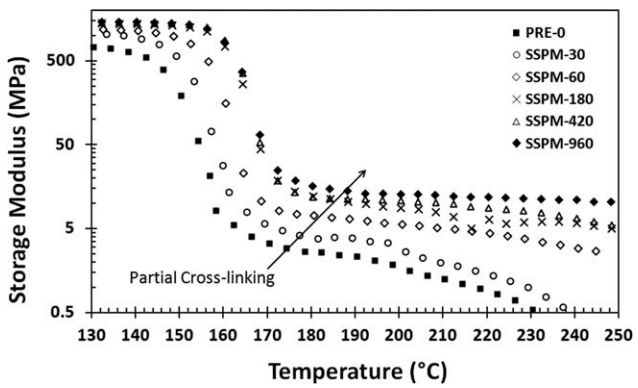

Figure 9. Behavior of storage modulus above the glass transition temperature (T_g) with different reaction time samples: PRE-0 (-■-), SSPM-30 (-○-), SSPM-60 (-◇-), SSPM-180 (-×-), SSPM-420 (-△-), and SSPM-960 (-◆-).

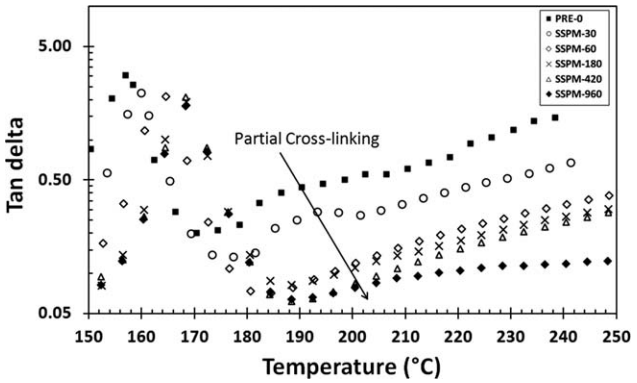

Figure 10. Behavior of loss tangent (tan δ) above the glass transition temperature (T_g) with different reaction time samples: PRE-0 (■), SSPM-30 (○), SSPM-60 (◇), SSPM-180 (×), SSPM-420 (△)), and SSPM-960 (◆)).

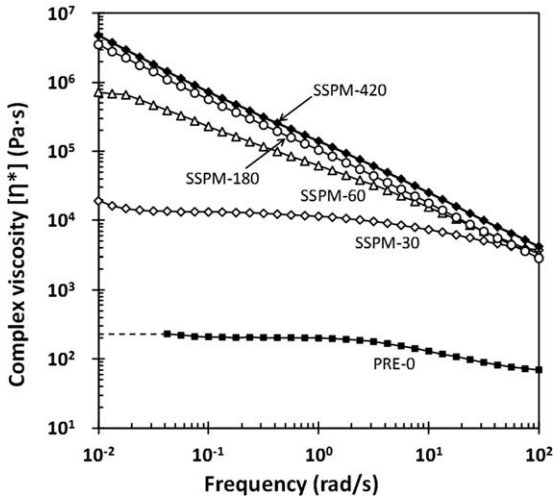

Figure 11. Dynamic viscosity of prepolymer and SSP_m PCs over a frequency range of 0.01–100 rad s^{-1}. SSP_m PC samples were prepared at 230°C with 10 μm thickness: PRE-0 (■), SSPM-30 (◇),SSPM-60 (△),SSPM-180 (○),SSPM-420 (◆)).

that the polymer loss moduli increases at a higher rate than the decreasing of the storage moduli, as chains are relaxed at higher temperatures. When the density of partial crosslinks increases with reaction time, tan δ decreases at each given analysis temperature indicating that energy loss becomes lower. SSPM-960 shows a rubber elastic plateau at temperatures above 220°C.

Rheological Properties. The rheological properties of the soluble fraction of polycarbonates have been characterized above the polymer's melting temperature (T_m). Because SSP_m PCs have branched and partially crosslinked chemical structures, the flow properties enable us to further understand the microstructural characteristics of the polymer. In general, higher molecular weight polymers have lower flow property.[10,36–39] However, flowability of nonlinearly structured polymers such as branched and crosslinked polymers depends not only on the molecular weight but also on the degree of branching and crosslinking.[40,41] The 10-μm-thick high molecular weight polycarbonate samples obtained by SSP_m were fused to prepare 400–500 μm thickness samples prior to the rheological measurement. A strain of 5% was used in the experiments at 260°C[29,30] that is ~10°C higher for the polymer chain disentanglement (see Figure 10) observed in DMA results. Dynamic storage (G'), loss shear moduli (G'), and complex viscosity (η^*) were obtained at a frequency range of 0.01–100 rad s^{-1} under the continuous nitrogen gas flow to prevent side reactions.

The complex viscosities of linear prepolymer (sample PRE-0) and high molecular weight nonlinear SSP_m PCs (SSPM-xxx) are shown in Figure 11. The prepolymer sample PRE-0 behaves like a typical Newtonian liquid. As molecular weight is increased with branching and partial crosslinking, zero shear viscosities increase by two orders of magnitude (e.g., sample SSPM-30). The shear thinning effect does not change much for the sample obtained after 30 min of reaction (sample SSPM-30). For longer reaction time (e.g., SSPM-60), the complex viscosity increases

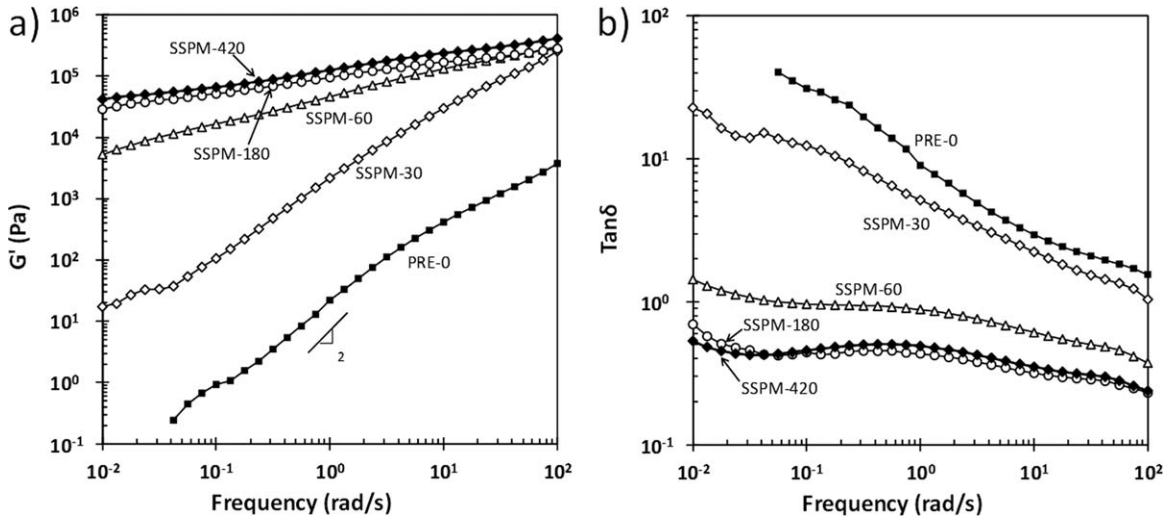

Figure 12. (a) Shear storage modulus (G') and (b) loss tangent (tan δ) of prepolymer and SSP_m PCs over a frequency range of 0.01–100 rad s^{-1}. SSP_m PC samples were prepared at 230°C with 10 μm thickness: PRE-0 (■), SSPM-30 (◇),SSPM-60 (△)),SSPM-180 (○),SSPM-420 (◆).

and the range of the zero shear rate for Newtonian region becomes very narrow. For the SSPM-180 and SSPM-420, the Newtonian behavior is not observed in the frequency range of 0.01–100 rad s^{-1}. It has been reported that molecular weight, molecular structure, and polymer relaxation rate affect the degree of shear thinning.[10,42] Decreased polymer chain relaxation or diffusion rate for high molecular weight nonlinear polycarbonates with branching and partial crosslinking give rise to higher shear thinning effect.[10,42] Linear viscoelastic behaviors were observed for the SSPM-180 and SSPM-420 which contain about 5 and 49% insoluble gel, respectively. For the SSPM-420 (49% insoluble gel), a slight increase of shear viscosity is observed in comparison with the SSPM-180. It is reported that the relaxation time of the crosslinked polymers near gel point becomes large and therefore, steady shear flow is not reached.[43]

Figure 12(a) shows shear storage modulus (G') of prepolymer and SSP_m PCs over a frequency range of 0.01–100 rad s^{-1}. For the sample PRE-0 (linear low molecular weight polycarbonate), the storage modulus (G') decreases as frequency decreases and the slope is ~2.0 which represents a typical behavior of Newtonian fluids. For the SSPM-30, storage modulus increases by about two orders of magnitude but the slope is nearly the same. In addition, loss modulus values are higher than the storage modulus for all the frequency range in that tan δ values are higher than 1.0 [see Figure 12(b)]. The sample SSPM-30 has insoluble fraction below 1 wt %. As insoluble fraction increases with reaction time (>180 min), the complex viscosity (as shown in Figure 11) and storage modulus [as shown in Figure 12(a)] show more rubber-like behavior in that zero shear viscosity is not observed and the slope of storage modulus approaches zero.[40–42] Recall that in the ^{1}H NMR data, the mole fractions of crosslinked polymers are 3.55×10^{-4}, 8.89×10^{-4}, and 4.26×10^{-2} for the reaction times of 30, 60, and 180 min, respectively (see Table I). As the amount of crosslinked polycarbonates increases in micro-layers, the storage modulus (G') increases faster than the loss modulus (G'), indicating that melt elasticity of partially crosslinked polycarbonate is much higher than the low molecular weight linear prepolymer (PRE-0) and the samples with smaller amount of crosslinks [Figure 12(b)]. For the SSPM-180 and SSPM-420 samples, the storage modulus is larger than the loss modulus at all frequency range tested in our experiments.

CONCLUDING REMARKS

In this article, we have reported the synthesis of high molecular weight polymers with nonlinear molecular structures due to branching and partial crosslinking reactions in the solid-state polymerization of polycarbonates in micro-layers. The polymerization in micro-layers offers unique phenomena of radical-induced partial crosslinking reactions due to the rapid removal of phenol. The micro-layer thickness was such that phenol diffusion resistance was practically absent and as a result, the radicals generated by chain scission and hydrogen abstraction reactions were able to engage in further reaction without reacting with phenol. When the degree of cross-linking was low, some of these polymers dissolved in the solvent, indicating that the cross-linking did not occur globally but locally to enable the dissolution of the polymer in solvents. We have observed that as the polymerization in micro-layers continued to 960 min, the mass fraction of insoluble polymers becomes nearly 95% while the entire mass of the polymer micro-layers remain optically clear with no sign of discoloration. The thermal, mechanical, and rheological properties of high molecular weight polycarbonates were also investigated by DSC, DMA, and rheological analysis. It has been observed that the glass transition temperature increased to about 159°C after 180 min of reaction and it was concluded that the glass transition temperature was no longer affected by the degree of cross-linking afterward. However, the peak height of the loss tangent curve decreased as the reaction time of SSP_m process increases (up to 960 min), indicating that the energy loss (phase lag (δ)) decreased as molecular weight of polymer increased due to crosslinking. These phenomena were confirmed by the DMA using temperature sweep mode. The sample containing 95% insoluble gel (960 min) showed the rubber elastic plateau in both storage modulus and tan δ versus temperature profiles. For longer SSP_m reaction times, the storage modulus increased and the slope decreased reaching a plateau. The rheological analysis of the nonlinear polymer samples indicated that shear thinning effect was promoted as branching and partial crosslinking reactions increased in the SSP_m process. With an increase in the insoluble fraction, the storage modulus becomes much larger than the loss modulus, indicating that these polycarbonates are quite different class of polycarbonates from conventional linear and low molecular weight polycarbonates. The experimental findings from this work can be applied to *in situ* formation of high molecular weight nonlinear polycarbonate through, for example, a continuous film formation and reaction process.

ACKNOWLEDGMENTS

The authors acknowledge the financial support by the National Science Foundation (NSF-CBET Award No. 1033071). We also acknowledge the technical support by Dr. Yiu-Fai Lam at the Department of Chemistry and Biochemistry at the University of Maryland for their assistance in analyzing the reaction products.

REFERENCES

1. DeRudder, J. L. In Commercial Applications of Polycarbonate; Legrand, D. G., Bendler, J. T., Eds.; Marcel Dekker: New York, **2000**; p 303.
2. Brunelle, D. J. Advances in Polycarbonates; ACS Symposium Series 626; American Chemical Society: Washington, DC, **2005**; p 1.
3. Zhai, W.; Yu, J.; Ma, W.; He, J. *Macromolecules* **2007**, *40*, 73.
4. Marks, M. J.; Sekinger, J. K. *Macromolecules* **1994**, *27*, 4106.
5. Boonstra, T. O.; Olden, D. V.; Woudenberg, R. H.U.S. Pat. 5,908,916 A, **1999**.
6. Lee, H. K.; Yuko, Y.; Kim, K. Y. U.S. Pat. 7,297,452 B292, **2007**.
7. Karlik, D.; Brack, H. P.; Verhoogt, H.; Lemmon, J. P.; Kamps, J. H.; Sederel, W. L.; Goossens, J. M. D. U.S. Pat. 6504002 B6504001, 650, **2003**.

8. Hagenaars, A. C.; Pesce, J. J.; Bailly, C.; Wolf, B. A. *Polymer* **2001**, *42*, 7653.
9. Marks, M. J.; Munjal, S.; Namhata, S.; Scott, D. C.; Bosscher, F.; De Letter, J. A.; Klumperman, B. *J. Polym. Sci. A Polym. Chem.* **2000**, *38*, 560.
10. Lyu, M. Y.; Lee, J. S.; Pae, Y. *J. Appl. Polym. Sci.* **2001**, *80*, 1814.
11. Davis, A.; Golden, J. H. *Nature* **1965**, *206*, 397.
12. Davis, A.; Golden, J. H. *Makromol. Chem.* **1967**, *110*, 180.
13. Woo, B. G.; Choi, K. Y.; Song, K. H. *Ind. Eng. Chem. Res.* **2001**, *40*, 1312.
14. Kim, Y.; Choi, K. Y. *J. Appl. Polym. Sci.* **1993**, *49*, 747.
15. Davis, A.; Golden, J. H. *Makromol. Chem.* **1964**, *78*, 16.
16. Oba, K.; Ishida, Y.; Ito, Y.; Ohtani, H.; Tsuge, S. *Macromolecules* **2000**, *33*, 8173.
17. McNeill, I. C.; Rincon, A. *Polym. Degrad. Stabil.* **1991**, *31*, 163.
18. Montaudo, G.; Puglisi, C.; Samperi, F. *Polym. Degrad. Stabil.* **1991**, *31*, 291.
19. Fukuoka, S.; Watanabe, T.; Dozono, T. U.S. Pat. 4, 948, 871, **1990**.
20. Shi, C.; DeSimone, J. M.; Kiserow, D. J.; Roberts, G. W. *Macromolecules* **2001**, *34*, 7744.
21. Shi, C.; Gross, S. M.; DeSimone, J. M.; Kiserow, D. J.; Roberts, G. W. *Macromolecules* **2001**, *34*, 2060.
22. Ye, Y.; Choi, K. Y. *Polymer* **2008**, *49*, 2817.
23. Ye, Y.; Choi, K. Y. *Macromol. React. Eng.* **2010**, *4*, 613.
24. Baick, I. H.; Ye, Y.; Luciani, C. V.; Ahn, Y. G.; Song, K. H.; Choi, K. Y. *Ind. Eng. Chem. Res.* **2013**, *52*, 17419.
25. Kim, Y.; Choi, K. Y.; Chamberlin, T. A. *Ind. Eng. Chem. Res.* **1992**, *31*, 2118.
26. Foti, M.; Ingold, K. U.; Lusztyk, J. *J. Am. Chem. Soc.* **1994**, *116*, 9440.
27. Valdebenito, A.; Lissi, E. A.; Encinas, M. V. *Macromol. Chem. Phys.* **2001**, *202*, 2581.
28. Oba, K.; Ishida, Y.; Ohtani, H.; Tsuge, S. *Polym. Degrad. Stabil.* **2002**, *76*, 85.
29. Xu, L.; Weiss, R. A. *Macromolecules* **2003**, *36*, 9075.
30. Delbreilh, L.; Dargent, E.; Grenet, J.; Saiter, J. M.; Bernes, A.; Lacabanne, C. *Eur. Polym. J.* **2007**, *43*, 249.
31. van Melick, H. G. H.; Govaert, L. E.; Meijer, H. E. H. *Polymer* **2003**, *44*, 2493.
32. Mulliken, A. D.; Boyce, M. C. *J. Eng. Mater. Technol.* **2006**, *128*, 543.
33. Fox, T. G.; Flory, P. J. V. *J. Am. Chem. Soc.* **1948**, *70*, 2384.
34. Fox, T. G.; Flory, P. J. *J. Appl. Phys.* **1950**, *21*, 581.
35. Fox, T. G.; Flory, P. J. *J. Phys. Chem.* **1951**, *55*, 221.
36. Folt, V. L. *Rubber Chem. Technol.* **1969**, *42*, 1294.
37. Schaefgen, J. R.; Flory, P. J. *J. Am. Chem. Soc.* **1948**, *70*, 2709.
38. Masuda, T.; Ohta, Y.; Onogi, S. *Macromolecules* **1971**, *4*, 763.
39. Romani, F.; Corrieri, R.; Braga, V.; Ciardelli, F. *Polymer* **2002**, *43*, 1115.
40. Winter, H. H. *Progr. Colloid* & Polym. Sci. **1987**, *75*, 104.
41. Tian, J.; Yu, W.; Zhou, C. *Polymer* **2006**, *47*, 7962.
42. Al-Muntasheri, G. A.; Hussein, I. A.; Nasr-El-Din, H. A.; Amin, M. B. *J. Petrol. Sci. Eng.* **2007**, *55*, 56.
43. Brunelle, D. J.; Kailasam, G. Polycarbonate. GE Technical Information Series, internal report, **2002**; 2001CRD136.